

Cell-strain-energy costs of active control of contractilityJosephine Solowiej-Wedderburn and Carina M. Dunlop^{*}*School of Mathematics and Physics, University of Surrey, Guildford GU2 7XH, United Kingdom*

(Received 22 August 2022; accepted 8 June 2023; published 21 June 2023)

Cell mechanosensing is implicated in the control of a broad range of cell behaviors, with cytoskeletal contractility a key component. Experimentally, it is observed that the contractility of the cell responds to increasing substrate stiffness, showing increased contractile force and changing the distribution of cytoskeletal elements. Here, we show using a theoretical model of active cell contractility that upregulation of contractility need not be energetically expensive, especially when combined with changes in adhesion and contractile distribution. Indeed, we show that a feedback mechanism based on the maintenance of strain energy would require an upregulation in contractile pressure on all but the softest substrates. We consider both the commonly reported substrate strain energy and active work done. We demonstrate substrate strain energy would preferentially select for the experimentally observed clustering of cell adhesions on stiffer substrates which effectively soften the substrate and enable an upregulation of total contractile pressure, while the localization of contractility has the greatest impact on the internal work.

DOI: [10.1103/PhysRevE.107.L062401](https://doi.org/10.1103/PhysRevE.107.L062401)

It is well established that cells sense, adapt, and respond to the mechanical properties of their environment. This mechanosensing is key across cell behaviors, ultimately affecting, e.g., cell growth, development, and differentiation [1–3]. Fundamental to mechanosensing are contractile forces generated by myosin motors within an actin rich network in the cell. These forces are transmitted from the cell to the extracellular matrix through adhesions [4]. A focus of mechanotransduction research has traditionally been these sites of cell adhesion, which in stiffer environments are concentrated into small patches of strong attachment called focal adhesions [1,3].

Experimental investigations commonly use engineered gels or micropillar arrays with defined mechanical properties to observe cell response [5]. As well as changes in signal transduction, changes in structural elements associated with cellular contractility are observed, including increased actin density and stress fiber formation [6,7]. Considering contractile forces, myosin and motor activity has been found to be more broadly distributed on soft gels becoming more localized, eventually overlapping with a dense actin cortex on stiffer substrates [8]. Hence it is typically observed that contractile forces increase with increased gel stiffness [9]. The mechanism by which stiffness changes lead to changes in contractile force is unclear although target stress or strain states are often implicated [10,11].

To quantify the mechanical activity of cells on two-dimensional substrates different approaches have been

suggested. Most commonly the applied tractions are measured, through, e.g., traction force microscopy, and used to infer activity. Recent work has suggested that the substrate strain energy could be effectively used as a measure for overall mechanical activity [12,13], leading to the observation that cells may respond directly to changes in substrate strain energy [14]. Substrate strain energy has also been observed to be approximately conserved across a range of stiffnesses [15], suggesting mechanical feedback to actively control strain energy. Even without fully constraining the strain energy, it is clear that there are bounds on the energy budget [16], with a link between cell contractility and energy consumption demonstrated [17]. Theoretically models have explored this energy budget using energy constraints as drivers of differentiation [18] or cell shape control [19].

We here use an active matter model to investigate both the substrate strain energy and the work done by the active cell components. We show that over a broad range of stiffnesses upregulation of active contractile pressure does not require an increase in energy expenditure. Indeed, upregulation of contractility is compatible with constant strain energy. We also investigate the localization of contractility into the cell cortex showing that this will have a minimal effect on the substrate strain energy at realistic levels of cell adhesion, although the active strain energy is sensitive to these changes. This is consistent with the observation that the localization of contractility can lead to large internal strains [20]. Introducing localized patches of adhesions, we see that these generate polarized cells, with the clustering of adhesion points particularly energetically favorable in terms of substrate strain energy, thus enabling significantly higher total contractile pressure.

Active matter model. Active matter models consider the cell as an elastic material with an additional component of stress generated by active contraction. Active contraction may be modeled either through computational simulations of

*c.dunlop@surrey.ac.uk

Published by the American Physical Society under the terms of the [Creative Commons Attribution 4.0 International](https://creativecommons.org/licenses/by/4.0/) license. Further distribution of this work must maintain attribution to the author(s) and the published article's title, journal citation, and DOI.

cytoskeletal filaments [21–23] or via a continuum approach [24–26]. We adopt the continuum approach taking the stress within the cell $\sigma = \sigma^P + \sigma^A$, where σ^P is the passive cell elasticity and σ^A is the active stress generated by the contractile pressure. Noting that the timescale for cell adhesion is faster than the relaxation timescale, viscoelastic effects may be neglected and we assume a linear elastic response in both the substrate and the cell (see, e.g., Ref. [26]). Furthermore, as the dimension of the spread cell is greater than its height h we consider planar deformations only. The constitutive relation for stress is thus $\sigma_{ij}^P = \frac{hE_c}{1+\nu}(\epsilon_{ij} + \frac{\nu}{1-\nu}\epsilon_{kk}\delta_{ij})$, with E_c the cell Young's modulus and ν the Poisson's ratio, and with $\sigma_{ij}^A = \frac{-hE_c}{2(1-\nu)}P\delta_{ij}$, assuming isotropic contractility. The phenomenological function P couples the activity of the contractile machinery to the active stress. This function may be conceptualized in different ways. Functionally, we see that when no forces are acting on the cell, including no adhesion between the cell and substrate $P = \epsilon_{kk}$, so that P is the net area change of material elements. Thus P quantifies the “target” strain of the cell system, and as such represents the maximal strain the system can exhibit in the absence of attachment [10]. In active gel models, P is typically interpreted in terms of a chemical potential of ATP and its reaction products [27]. In the context of the adherent cells considered as here, given the current understanding of how GTPases from the Rho family control contractility [11], it could equally be instructive to formulate the function P to correlate to, e.g., RhoA activity if this is quantified.

We here consider, in contrast to, e.g., Ref. [28], the role of this contractile force in determining the strain energy of the system. Thus we consider P as a control parameter in the system also considering a spatially nonuniform distribution of contractility. There are two strain energies that we focus on. These are derived from the work done to the substrate W_S , and the input of contractile work from the network of myosin motors which (from the conversion of ATP) are assumed generate the active work W_{CA} . The energies W_{CA} and W_S can be calculated from the deformations as

$$W_{CA} = \frac{1}{2} \int_A \sigma_{ij}^A \epsilon_{ij} dA, \quad W_S = \frac{1}{2} \int_A KT(\mathbf{x}) \mathbf{u} \cdot \mathbf{u} dA,$$

where the integrals are taken over the cell area A .

To determine the strain energies we calculate the cellular stresses, cell deformations, and applied tractions from the in-plane force balance over the cell

$$\nabla \cdot \sigma - T(\mathbf{x})K\mathbf{u} = \mathbf{0}, \quad (1)$$

with zero stress imposed at the cell boundary. The resistance of the substrate to deformation is here modeled as $-K\mathbf{u}$, with K the substrate stiffness. This is a common first-order approximation for thin gel substrates [24,29–31], where deformations are localized near the sites of applied traction generating an approximately linear relationship between stress and deformation. In the case of micropillars [5] where the resisting stress is proportional to the pillar deflection, the relationship is exact. To account for nonuniform adhesion of the cell to the substrate we set $T(\mathbf{x}) = 1$ where the cell is adhered and $T(\mathbf{x}) = 0$ where it is not. In the case of uniform adhesion [$T(\mathbf{x}) \equiv 1$] we recover the force balance of Refs. [24,29]. We here follow Ref. [28] and consider the two further cases for

$T(\mathbf{x})$ of a cell adhered over a ring and of adhesions in spots mimicking focal adhesions, imposing the continuity of stress and deformation at internal boundaries [28].

The substrate strain energy W_S is experimentally measurable and is often reported as a measure of mechanical activity (see, e.g., Refs. [12–15]). The active work done W_{CA} is also clearly important as it can be conceptually linked to the energy required to drive the cell into its contractile state, with hard constraints on its possible size [16]. However, W_{CA} is significantly harder to directly experimentally quantify than W_S and to interpret. These energies are complemented by a third energy $W_P = \frac{1}{2} \int_A \sigma_{ij}^P \epsilon_{ij} dA$, which represents the work done to the passive elements of the cell. As there is no net change in energy $W_{CA} + W_S + W_P = 0$, hence it is sufficient to consider two energies with W_P the least experimentally accessible quantity.

Uniform and isotropic contractile pressure. We first consider that contractility is uniform throughout the cell. We consider two arrangements of adhesion: uniform adhesion to the substrate, and adhesion within a circular annulus. In these cases, with $P = -P_0$ constant, the cell deformations may be analytically determined (see Supplemental Material [32] for the calculation). In the case $T(\mathbf{x}) \equiv 1$, W_S and W_{CA} are calculated from the deformations as

$$\widehat{W}_{CA} = -\frac{\pi P_0^2(1+\nu)^2}{4(\nu-1)\left(\frac{\gamma}{\nu-1}\frac{I_0(\gamma)}{I_1(\gamma)} + 1\right)},$$

$$\widehat{W}_S = \frac{\pi P_0^2(1+\nu)^2 \left\{ I_0(\gamma)I_1(\gamma) - \frac{\gamma}{2}[I_0(\gamma)^2 - I_1(\gamma)^2] \right\}}{4\gamma \left(I_0(\gamma) + \frac{\nu-1}{\gamma} I_1(\gamma) \right)^2},$$

where $\widehat{W}_x = [(1-\nu^2)/hE_c r_0^2]W_x$, and $I_{0,1}$ are modified Bessel functions. $\gamma^2 = K(1-\nu^2)r_0^2/hE_c$ is the key nondimensional control parameter, which quantifies the relative stiffness of the cell and substrate for a cell of diameter $2r_0$. Stiffer gels correspond to larger γ . These expressions relate the strain energies to the contractile pressure required to do the respective work.

We consider first the active strain energy W_{CA} . The term $tI_N(t)/I_{N+1}(t)$ is a monotone increasing function for $t > 0$ (see Ref. [33]), and so as the relative substrate stiffness increases (γ increases), W_{CA} decreases in magnitude. Thus it is possible to upregulate the contractility P_0 on stiffer substrates without increasing the energy expenditure. Indeed, if the energy W_{CA} is constrained to be approximately constant, this necessitates an increase in contractility. This can be seen in the strain-energy heat map [Fig. 1(a)], where the contours of constant strain energy demonstrate the positive correlation between substrate stiffness and contractility.

For W_S , for any fixed γ increasing contractility increases the substrate strain energy, as also observed experimentally in Ref. [11], where optogenetic upregulation of contractility generated an increase in substrate strain energy. As γ varies we see similar results as for W_{CA} across larger values of γ so that again increasing γ without upregulating contractility would generate a decrease in energy. This can be conceptualized broadly in the context of a two spring model of cell-substrate mechanics (see, e.g., Refs. [34,35]), where the cell and substrate are thought of as springs in series so that the strain energy of the system is $W_S = F^2/2K$, where K is the effective spring constant and F the applied force. In

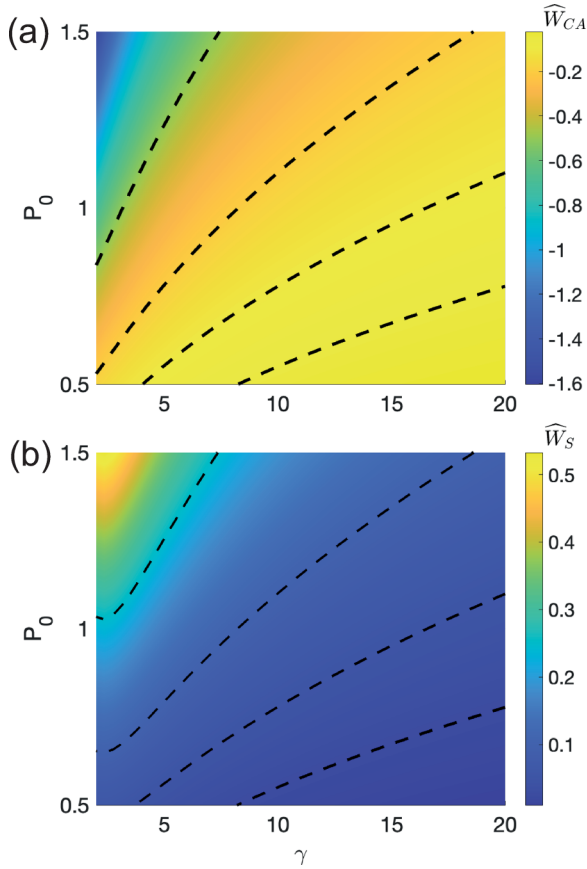


FIG. 1. Strain energy for a completely adhered cell with uniform contractility P_0 on substrate of stiffness γ . (a) Active strain energy \widehat{W}_{CA} , where dashed lines are contours at $\widehat{W}_{CA} = -0.5, -0.2, -0.1, -0.05$ from top to bottom. (b) Substrate strain energy \widehat{W}_S , where dashed lines are contours at $\widehat{W}_S = 0.25, 0.1, 0.05, 0.025$ from top to bottom.

this heuristic framework, increasing substrate stiffness thus decreases substrate strain energy for the same force. Although this is useful, in a fully two-dimensional continuum model the relationship between force and displacement is more complex. Indeed, on softer substrates we see that W_S now depends nonmonotonically on γ [Fig. 1(b)]. In Fig. 2 we plot two illustrative contours (solid lines) of the active strain energy and the substrate strain energy. These highlight the qualitatively different behaviours of the energy measures at low stiffnesses. For W_S it can be seen that on the softest substrates (e.g., $\gamma < 2.3$, completely adhered disk) increasing substrate stiffness requires contraction to be reduced to maintain the substrate strain-energy constant. Indeed, not reducing contractility would require the cell to do more work to the substrate on these softest substrates, and also to undergo large internal strains. As such it would clearly be practically favorable to select for lower contraction in these cases. As substrate stiffness increases so again the contractility may be upregulated on stiffer substrates at little or no energetic cost.

We consider now the scenario where adhesion is not complete between the cell and the substrate, looking at how the amount of adhesion affects the strain energy, specifically, adhesion in a ring so that $T(r) = 1$ in $r_1 < r < r_0$. In this case,

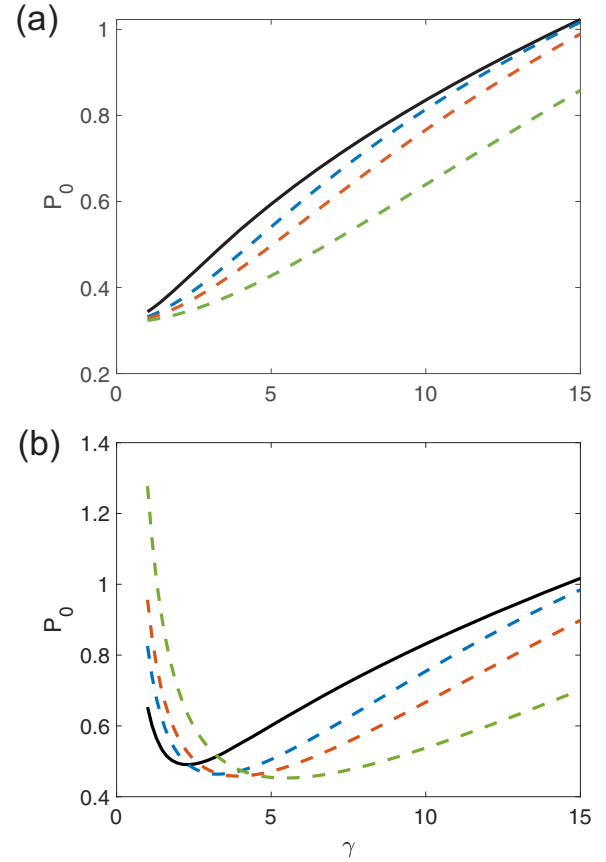


FIG. 2. Lines of constant (a) \widehat{W}_{CA} and (b) \widehat{W}_S against increasing substrate stiffness (γ increasing). Above each line more work is done and below less. The solid black line is for complete adhesion and blue, orange, and green dashed lines are adhesion at the rim at 30%, 20%, and 10% adhesion, respectively (corresponding to $r_1/r_0 = 0.84, 0.89, 0.95$, respectively). \widehat{W}_{CA} and \widehat{W}_S are -0.1154 and 0.057 , respectively.

similar analytical solutions may be obtained for W_S and W_{CA} in terms of γ and P_0 as before but with the annulus size r_1/r_0 an additional parameter, for example now,

$$\widehat{W}_{CA} = -\frac{\pi P_0^2 (1 + \nu)^2}{4\gamma} \frac{I_1(\gamma) + H(\gamma r_1/r_0)K_1(\gamma)}{F(\gamma) - H(\gamma r_1/r_0)G(\gamma)},$$

with

$$F(z) = I_0(z) + \frac{(\nu - 1)}{z} I_1(z),$$

$$G(z) = K_0(z) - \frac{(\nu - 1)}{z} K_1(z),$$

$$H(z) = \left(\frac{zI_0(z) - 2I_1(z)}{zK_0(z) + 2K_1(z)} \right).$$

See Supplemental Material [32] for the calculation and corresponding formula for W_S . For an adhered ring, similar qualitative behavior is observed as for complete adhesion (see Fig. 2). However, reducing the percentage of the cell adhered to the substrate reduces the amount of contractile pressure required to do the same work due to the lower substrate resistance on all but the softest substrates. However, the reduction in adhesion needs to be significant before this effect is seen

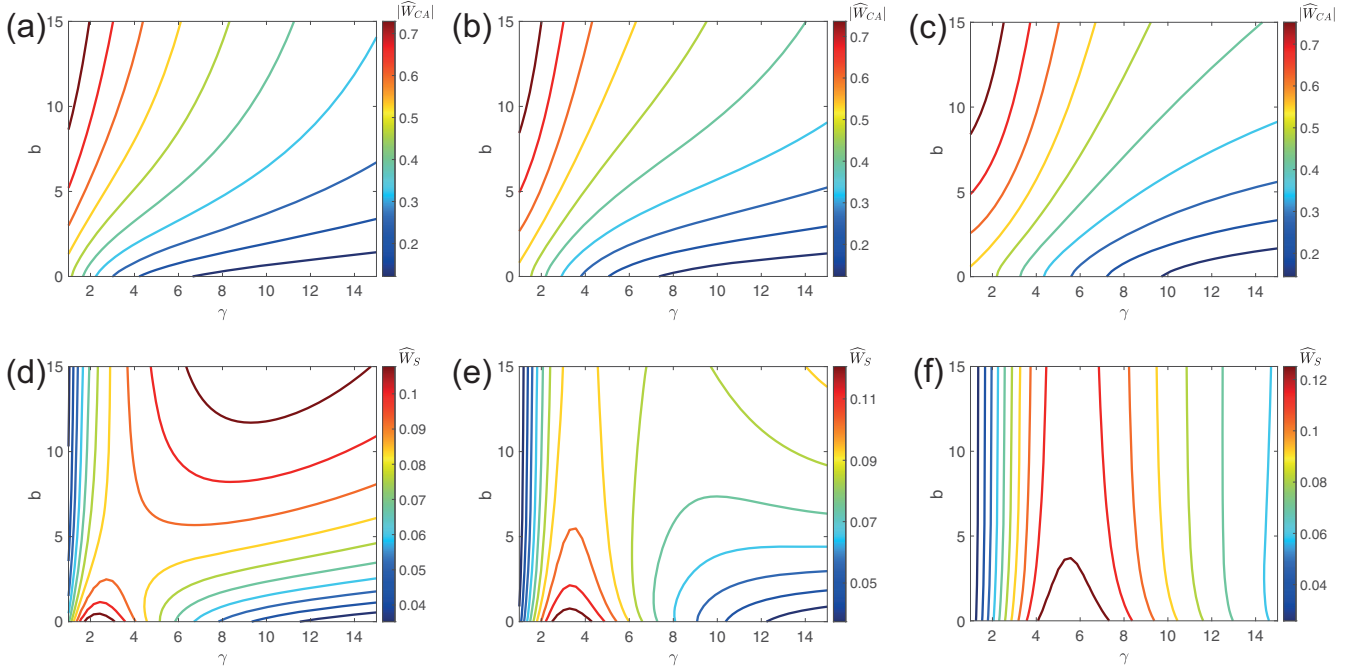


FIG. 3. (a)–(c) Contour plots of fixed \widehat{W}_{CA} : (a) complete adhesion; (b) 30% adhered ring; (c) 10% adhered ring. (d)–(f) Contour plots of fixed \widehat{W}_S : (d) complete adhesion; (e) 30% adhered ring; (f) 10% adhered ring. $P_0 = 0.7$ for all plots.

with even a ring covering 20% of the cell area still demonstrating very similar behavior to complete adhesion (see Fig. 2).

Spatially varying contractile pressure. It is experimentally observed that the contractile apparatus of cells is concentrated towards the cell edge [36,37]. Significantly the distribution of actin and myosin is observed to change in response to changes in stiffness, eventually concentrating in a thin, more active cortex on stiff substrates [8]. To explore how altering the spatial distribution of contractile elements affects the cell energy budget we consider $P = P(r)$, where r is the radial distance from the cell center. As in Ref. [20], we assume that $P(r)$ is a monotonic decreasing function so P generates greater contractility at the edge. For specificity, $P(r) = -a(1 + br^n)$, with $a, b > 0$, which is chosen for analytical convenience, with $n = 5$ ensuring a strong differential in the contractile pressure. We take $a = P_0(n + 2)/(n + 2 + 2br_0^n)$ so that total contractile pressure $\frac{-hE_c}{2(1-\nu)} \int_A P dA = \frac{hE_c \pi r_0^2 P_0}{2(1-\nu)}$ is the same as for uniform contractility. The parameter b adjusts the distribution of contractile elements, with increasing b corresponding to the localization of contraction to the cell edge. Provided the radial symmetry of the adhesion pattern is not broken, an analytical solution of a similar form is still available for the cell deformations and hence strain energies. However, in this case, the nonconstant P generates a nonhomogeneous equation so that the solution is expressed in terms of Struve functions rather than Bessel functions [38,39] (see Supplemental Material [32]).

In Figs. 3(a)–3(c), we set $P_0 = 0.7$ (which is consistent with the contractile moment reported in Ref. [40]) and plot contours of fixed active energy as γ and b are varied. We see that increasing the substrate stiffness without altering the distribution of contractility or total contractile pressure will inevitably generate a reduction in W_{CA} as expected. However,

we see by following contours that concentrating the contractility towards the edge of the cell (increasing b) can maintain W_{CA} . This is observed across a range of adhesion. Thus the concentration of contractility is playing a similar role to increased total contractility in terms of internal deformations and control of W_{CA} . However, in considering the substrate strain energy W_S a markedly different picture emerges [see Figs. 3(d)–3(f)]. Now depending on the localization factor substrate strain energy may increase or decrease as substrate stiffness increases. In this way at lower values of the localization factor the same nonlinear behavior is observed as for uniform contractility, as might be expected. As localization increases, we may need to either reduce or increase localization to maintain a constant energy depending on the starting stiffness. Significantly, as the adhesion percentage reduces, so the strain energy stored in the substrate becomes independent of the localization with at 10% adhesion almost complete decoupling. Thus localization as a mechanical component in mechanotransduction is likely most significant to internal stresses as has previously been suggested [20]. It is thus practically the case that the observed localization of contractile machinery would not result in an increase in observed substrate strain energy, consistent with the observations of Ref. [15].

Adhesion patterning. We finally consider adhesion in small localized patches to investigate the role of focal adhesions. We consider a pattern of 20 spots either evenly distributed around the cell edge [Fig. 4(a)], or alternatively in two clusters at opposite ends to generate polarized cell shapes [Fig. 4(b)]. In the case of adhered spots, analytical solutions cannot be obtained and we solve Eq. (1) using finite-element methods implemented in MATLAB 2019b [partial differential equation (PDE) toolbox]. Each spot has radius r_s , and radial position

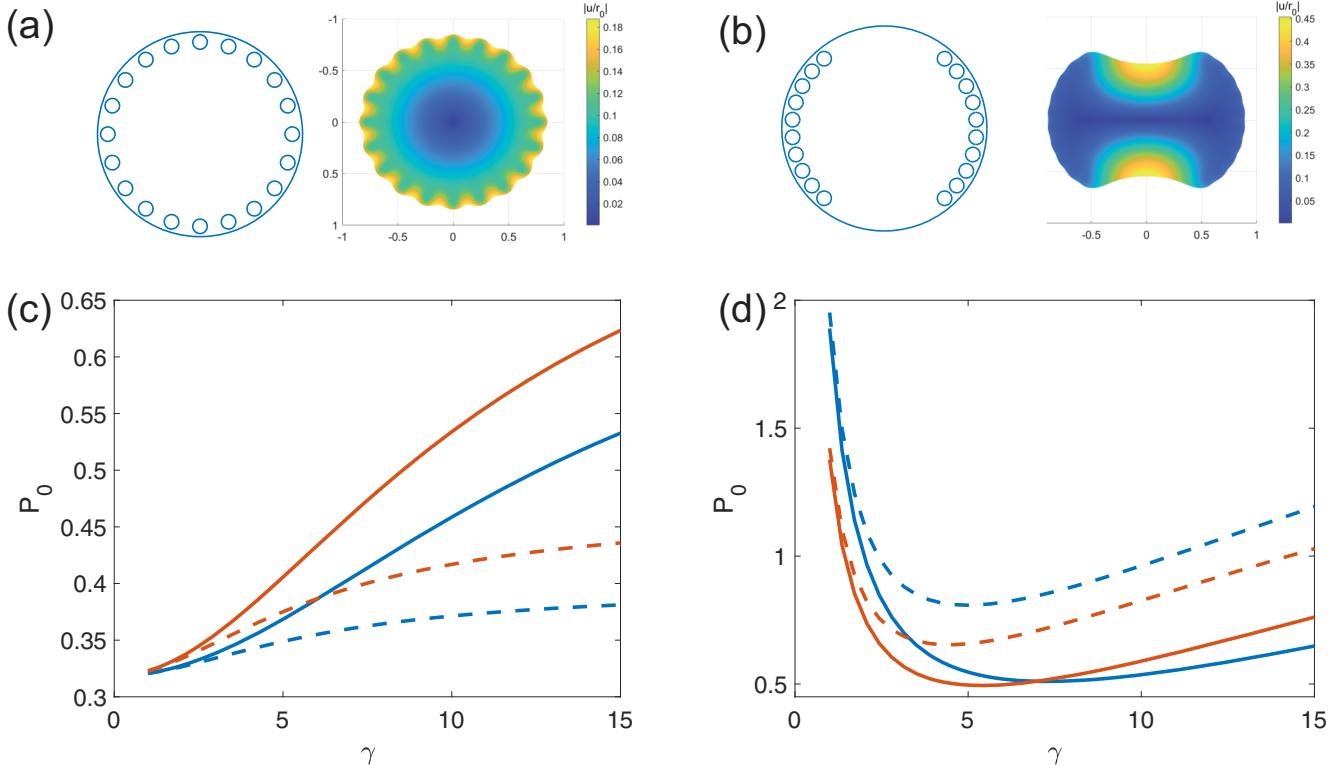


FIG. 4. (a) An adhesion pattern with 20 spots evenly distributed around the cell edge (10% adhered area) and the corresponding cell deformation ($\gamma = 7$, $P_0 = 0.7$). (b) An adhesion pattern with 20 spots distributed in two clusters and the resultant deformation ($\gamma = 7$, $P_0 = 0.7$). (c) and (d) Plots of total cellular contractility P_0 that maintain (c) fixed W_{CA} ($\widehat{W}_{CA} = -0.1154$) and (d) fixed W_S ($\widehat{W}_S = 0.057$) for adhesion patterns of 20 spots distributed either evenly (solid lines) or in two clusters (dashed lines) for two different spot sizes, 5% adhered area in blue, and 10% adhered area in orange.

$r_p = 0.98r_0 - r_s$. For an even distribution of spots, circles of adhesion were placed at angles $2\pi/20$. For two adhesion clusters at opposite poles, the angle between adjacent spots in the same cluster was given by $2 \arcsin[(r_s + 0.015r_0)/r_p]$. Each cluster had 10 spots, and the starting spots of each cluster were separated by angle π . See Supplemental Material [32] for numerical details.

As in the case of an adhered ring, for a given spot distribution, W_{CA} would naturally reduce on stiffer substrates while W_S has the same initial increase over the softest values and then reduction on stiffer [Figs. 4(c) and 4(d)]. As such, we see that over much of the stiffness range contractility can increase without energy penalty and indeed any feedback mechanism based on constraining energy changes would necessitate an increase in contractility. On the effectively softest substrates (with lowest γ and low adhesive fraction) the cell strains can approach P_0 (the imposed maximal strain), at least locally. Thus depending on the local value of P_0 nonlinear elastic responses could be expected although as a first approximation we maintain linear elasticity. We note that, as the energy argument would suggest in practice, cell contractility would likely reduce in these cases to prevent such large strains and to reduce the associated energy cost.

We observe significant differences in the effects of spot clustering on W_{CA} and W_S . Clustering of adhesions increases W_{CA} as larger cell deformations are incurred so that the possible contractility before energy increase is reduced (dashed

line), reducing possible increases in contractility. However, adhesion clustering reduces W_S so that this arrangement is energetically favorable in terms of substrate energy, as reported previously [28].

Significantly, experimental results suggest that adhesion distribution changes on stiffer substrates, resulting in more polarized cell shapes [40,41]. This experimentally observed behavior would be energetically favorable under a consideration of W_S [Fig. 4(d)], enabling greater upregulation of contractility, particularly on stiffer substrates. This further supports substrate strain energy as a useful correlative measure of mechanical activity, as suggested by, e.g., Ref. [14]. Additionally, we see that if we constrain substrate strain energy as per Ref. [15], this requires upregulation of contractile activity on stiffer substrates.

Conclusions. We have demonstrated both analytically and numerically that upregulating contractility on stiffer substrates need not be energetically expensive. Indeed, on stiffer substrates under the constraints of maintaining cell energy constant it is necessary for contractility to be increased to prevent a reduction in either the active energy or substrate energy on stiffer substrates. Significantly the experimentally observed localization of contractility to the cell edge has only a limited influence on substrate strain energy at realistic adhesion percentages. However, contractility localization does change the internal work done, in part due to the large internal strains that can be generated. This suggests that this behavior may be selected for by its influence on internal strain sensing

and internal structural reorganization. Significantly, we show that clustering of cell adhesions on stiffer substrates generate polarized cell shapes which are energetically favorable in terms of substrate strain energy, and enable significant contractile upregulation.

Acknowledgments. J.S.-W. acknowledges Ph.D. funding from the UK EPSRC, Institutional Doctoral Training Partnership (EP/N509772/1) and postdoctoral EPSRC funding (EP/W522302/1). C.M.D. also acknowledges financial support from the UK EPSRC (EP/M012964/1).

-
- [1] H. Wolfenson, B. Yang, and M. P. Sheetz, Steps in mechanotransduction pathways that control cell morphology, *Annu. Rev. Physiol.* **81**, 585 (2019).
- [2] A. J. Engler, S. Sen, H. L. Sweeney, and D. E. Discher, Matrix elasticity directs stem cell lineage specification, *Cell* **126**, 677 (2006).
- [3] A. Kumar, J. K. Placone, and A. J. Engler, Understanding the extracellular forces that determine cell fate and maintenance, *Development* **144**, 4261 (2017).
- [4] M. A. Wozniak and C. S. Chen, Mechanotransduction in development: A growing role for contractility, *Nat. Rev. Mol. Cell Biol.* **10**, 34 (2009).
- [5] W. J. Polacheck and C. S. Chen, Measuring cell-generated forces: A guide to the available tools, *Nat. Methods* **13**, 415 (2016).
- [6] J. Solon, I. Levental, K. Sengupta, P. C. Georges, and P. A. Janmey, Fibroblast adaptation and stiffness matching to soft elastic substrates, *Biophys. J.* **93**, 4453 (2007).
- [7] F. J. Byfield, R. K. Reen, T.-P. Shentu, I. Levitan, and K. J. Gooch, Endothelial actin and cell stiffness is modulated by substrate stiffness in 2D and 3D, *J. Biomech.* **42**, 1114 (2009).
- [8] B. A. T. Quang, R. Peters, D. A. D. Cassani, P. Chugh, A. G. Clark, M. Agnew, G. Charras, and E. Paluch, Extent of myosin penetration within the actin cortex regulates cell surface mechanics, *Nat. Commun.* **12**, 6511 (2021).
- [9] A. K. Yip, K. Iwasaki, C. Ursekar, H. Machiyama, M. Saxena, H. Chen, I. Harada, K.-H. Chiam, and Y. Sawada, Cellular response to substrate rigidity is governed by either stress or strain, *Biophys. J.* **104**, 19 (2013).
- [10] R. De, A. Zemel, and S. A. Safran, Do cells sense stress or strain? Measurement of cellular orientation can provide a clue, *Biophys. J.* **94**, L29 (2008).
- [11] T. Andersen, D. Wörthmüller, D. Probst, I. Wang, P. Moreau, V. Fitzpatrick, T. Boudou, U. Schwarz, and M. Balland, Cell size and actin architecture determine force generation in optogenetically activated cells, *Biophys. J.* **122**, 684 (2023).
- [12] S. Kollimada, F. Senger, T. Vignaud, M. Théry, L. Blanchoin, and L. Kurzawa, The biochemical composition of the actomyosin network sets the magnitude of cellular traction forces, *Mol. Biol. Cell* **32**, 1737 (2021).
- [13] A. Ghagre, A. Amini, L. K. Srivastava, P. Tirgar, A. Khavari, N. Koushki, and A. Ehrlicher, Pattern-based contractility screening, a reference-free alternative to traction force microscopy methodology, *ACS Appl. Mater. Interfaces* **13**, 19726 (2021).
- [14] V. Panzetta, S. Fusco, and P. A. Netti, Cell mechanosensing is regulated by substrate strain energy rather than stiffness, *Proc. Natl. Acad. Sci. USA* **116**, 22004 (2019).
- [15] P. W. Oakes, S. Banerjee, M. C. Marchetti, and M. L. Gardel, Geometry regulates traction stresses in adherent cells, *Biophys. J.* **107**, 825 (2014).
- [16] X. Yang, M. Heinemann, J. Howard, G. Huber, S. Iyer-Biswas, G. Le Treut, M. Lynch, K. L. Montooth, D. J. Needleman, S. Pigolotti, J. Rodenfels, P. Ronceray, S. Shankar, I. Tavassoly, S. Thutupalli, D. V. Titov, J. Wang, and P. J. Foster, Physical bioenergetics: Energy fluxes, budgets, and constraints in cells, *Proc. Natl. Acad. Sci. USA* **118**, e2026786118 (2021).
- [17] J. Xie, M. Bao, X. Hu, W. J. Koopman, and W. T. Huck, Energy expenditure during cell spreading influences the cellular response to matrix stiffness, *Biomaterials* **267**, 120494 (2021).
- [18] H. Suresh, S. S. Shishvan, A. Vigliotti, and V. S. Deshpande, Free-energy-based framework for early forecasting of stem cell differentiation, *J. R. Soc. Interface* **16**, 20190571 (2019).
- [19] V. Deshpande, A. DeSimone, R. McMeeking, and P. Recho, Chemo-mechanical model of a cell as a stochastic active gel, *J. Mech. Phys. Solids* **151**, 104381 (2021).
- [20] C. Dunlop, Differential cellular contractility as a mechanism for stiffness sensing, *New J. Phys.* **21**, 063005 (2019).
- [21] P. J. Albert and U. S. Schwarz, Modeling cell shape and dynamics on micropatterns, *Cell Adhes. Migr.* **10**, 516 (2016).
- [22] S. L. Freedman, S. Banerjee, G. M. Hocky, and A. R. Dinner, A versatile framework for simulating the dynamic mechanical structure of cytoskeletal networks, *Biophys. J.* **113**, 448 (2017).
- [23] S. S. Shishvan, A. Vigliotti, and V. S. Deshpande, The homeostatic ensemble for cells, *Biomech. Model. Mechanobiol.* **17**, 1631 (2018).
- [24] C. M. Edwards and U. S. Schwarz, Force Localization in Contracting Cell Layers, *Phys. Rev. Lett.* **107**, 128101 (2011).
- [25] S. Banerjee and M. C. Marchetti, Substrate rigidity deforms and polarizes active gels, *Europhys. Lett.* **96**, 28003 (2011).
- [26] B. M. Friedrich and S. A. Safran, How cells feel their substrate: Spontaneous symmetry breaking of active surface stresses, *Soft Matter* **8**, 3223 (2012).
- [27] J. Prost, F. Jülicher, and J.-F. Joanny, Active gel physics, *Nat. Phys.* **11**, 111 (2015).
- [28] J. Solowiej-Wedderburn and C. Dunlop, Sticking around: Cell adhesion patterning for energy minimization and substrate mechanosensing, *Biophys. J.* **121**, 1777 (2022).
- [29] S. Banerjee and M. C. Marchetti, Controlling cell-matrix traction forces by extracellular geometry, *New J. Phys.* **15**, 035015 (2013).
- [30] S. He, Y. Su, B. Ji, and H. Gao, Some basic questions on mechanosensing in cell-substrate interaction, *J. Mech. Phys. Solids* **70**, 116 (2014).
- [31] P. Marcq, N. Yoshinga, and J. Prost, Rigidity sensing explained by active matter theory, *Biophys. J.* **101**, L33 (2011).
- [32] See Supplemental Material at <http://link.aps.org/supplemental/10.1103/PhysRevE.107.L062401> for analytical solutions and details of numerical methods.
- [33] H. C. Simpson and S. J. Spector, Some monotonicity results for ratios of modified Bessel functions, *Q. Appl. Math.* **42**, 95 (1984).

- [34] U. S. Schwarz, T. Erdmann, and I. B. Bischofs, Focal adhesions as mechanosensors: The two-spring model, *BioSystems* **83**, 225 (2006).
- [35] L. Feld, L. Kellerman, A. Mukherjee, A. Livne, E. Bouchbinder, and H. Wolfenson, Cellular contractile forces are non-mechanosensitive, *Sci. Adv.* **6**, eaaz6997 (2020).
- [36] M. Murrell, P. W. Oakes, M. Lenz, and M. L. Gardel, Forcing cells into shape: The mechanics of actomyosin contractility, *Nat. Rev. Mol. Cell Biol.* **16**, 486 (2015).
- [37] P. Chugh and E. Paluch, The actin cortex at a glance, *J. Cell Sci.* **131**, jcs186254 (2018).
- [38] M. Abramowitz and I. A. Stegun, *Handbook of Mathematical Functions: With Formulas, Graphs, and Mathematical Tables*, Vol. 55 (Courier Corporation, North Chelmsford, MA, 1964).
- [39] L. J. Slater, *Generalized Hypergeometric Functions* (Cambridge University Press, Cambridge, UK, 1966).
- [40] M. Prager-Khoutorsky, A. Lichtenstein, R. Krishnan, K. Rajendran, A. Mayo, Z. Kam, B. Geiger, and A. D. Bershadsky, Fibroblast polarization is a matrix-rigidity-dependent process controlled by focal adhesion mechanosensing, *Nat. Cell Biol.* **13**, 1457 (2011).
- [41] B. Geiger, J. P. Spatz, and A. D. Bershadsky, Environmental sensing through focal adhesions, *Nat. Rev. Mol. Cell Biol.* **10**, 21 (2009).